African Journal of Biological Sciences

Journal homepage: http://www.afjbs.com

Research Paper   Open Access

Fabrication of Novel Nanofiber Patch Containing BoerhaviaDiffusa Extract for Wound Healing Application Using Response Surface Methodology

Smita Borkar[1*], Hemant kumar Yadav[1], Abhay Raizaday[2]

[1]School of Pharmacy, Suresh Gyanvihar University, Jaipur, Rajasthan, [2]Department of Pharmaceutics, college of pharmacy, JSS Academy of Technical Education, Noida-62.

[*]**Corresponding Author -Mrs. Smita Borkar**

Author Affiliation-School of Pharmacy, Suresh Gyanvihar University, Jaipur, Rajasthan

E-mailID:smita.borkaragcop@gmail.com

Abstract:

In this study, we successfully prepared a Boerhavia diffusa extract-loaded nanofiber wound dressing using the electrospinning method, optimizing the process through a 3x2 factorial design. The optimized nanofiber, denoted as BRNF7, exhibited excellent characteristics, including an entrapment efficiency of 85.12% and a drug loading of 9%. Furthermore, the swelling index was measured at 86.6, demonstrating its potential as an effective wound dressing material. Characterization of the BRNF7 nanofiber revealed promising results, as FTIR spectra exhibited all the expected peaks, while XRD analysis indicated a highly crystalline structure with intense peaks. DSC thermograms displayed a characteristic peak at 133.42°C, corresponding to Boerhavia diffusa extract. Thermal analysis, as indicated by TGA thermograms, showed that the nanofiber gradually decomposed at a higher temperature range, signifying its thermal stability. Wound dressing various parameter included as the film thickness ranged from 0.069 to 0.074 mm, and all films exhibited excellent folding endurance, ensuring flexibility. Moisture interaction studies demonstrated good physical stability of the film under high humidity conditions and maintained integrity under dry conditions. The films exhibited a moisture absorption range of 3.8% to 4.6% and a moisture loss range of 3.2% to 4.7%. Tensile strength values ranged from 2.14 to 2.85 kg/cm², and the percentage of drug content was uniform between 90.15% and 92.11%.Furthermore, our Boerhavia diffusa extract-loaded Nanofibrous dressing displayed notable antibacterial activity against various pathogens and exhibited promising wound-healing effects, making it a potential candidate for advanced wound care. This study provides a comprehensive assessment of the BRNF7 nanofiber, emphasizing its potential in biomedical applications.

Keyword:wound healing, Nanofiber, electrospinning method, 32Factorial design

INTRODUCTION:

A wound is defined as the breakage in the continuity of the skin.). In general, wound healing is classified with four specific stages of hemostasis, inflammation, proliferation, and maturation [1-4] Wound healing is a complex biological process that is essential for the restoration of tissue integrity and function. Impaired wound healing can lead to chronic wounds, infections, and a reduced quality of life for affected individuals. Over the years, extensive research has been conducted to develop innovative strategies and materials that can enhance the wound healing process. [5-8]One such approach is the use of nanofiber-based wound dressings, which offer several advantages, including high surface area-to-volume ratio, excellent mechanical properties, and the capacity to encapsulate bioactive agents for controlled and sustained release. This article discusses the fabrication of novel nanofiber containing Boerhavia Diffusa extract, a traditional medicinal plant with documented wound healing properties, using 3^2,factorial design Response Surface Methodology (RSM).Boerhavia Diffusa, commonly known as "Punarnava" or "Hogweed," is a plant with a rich history in traditional medicine systems, such as Ayurveda and Traditional Chinese Medicine. It has been extensively studied for its various bioactive compounds, including alkaloids, flavonoids, and saponins, which possess anti-inflammatory, antioxidant, antimicrobial, and wound healing properties. Several studies have highlighted the potential of Boerhavia Diffusa extract in promoting angiogenesis, collagen synthesis, and epithelialization, making it a promising candidate for wound healing applications.[9-10]Nanofiber-based wound dressings have gained significant attention in recent years due to their unique structural and functional characteristics. These materials, often fabricated using electrospinning techniques, mimic the natural extracellular matrix, providing an ideal microenvironment for cells involved in wound healing. Nanofiber wound dressings offer enhanced moisture retention, breathability, and protection against external contaminants, making them suitable for various wound types, including chronic wounds, burns, and surgical incisions. [11-14]the objective of this study is to fabricate novel nanofiber wound dressings incorporating Boerhavia Diffusa extract using Response Surface Methodology (RSM). The research aims to optimize the electrospinning process parameters and characterize the resulting nanofiber for their morphology, mechanical properties, drug encapsulation efficiency, and sustained release of bioactive compounds. The ultimate goal is to develop an innovative wound dressing that harnesses the therapeutic potential of Boerhavia Diffusa for enhanced wound healing

MATERIAL AND METHOD:

Boerhavia Diffusa root, chloroform. Ethanol,PVA and PEO

FORMULATION DEVELOPMENT

***BORRAVIA DIFFUSA*EXTRACT LOADED NANOFIBER**

Active Methanolic extract of plant root (0.4 mg/ml.) was dissolved in PVA and PEO solution at the concentrations of 8mg/ml. The solution was stirred for 72 hours at room temperature, allowing all solid components to completely solubilize. At the given concentration, extracts dissolved rapidly to produce a translucent solution of uniform color and viscosity. The solution was electrospun into solid fiber mats under the following conditions: 20 kV DC offset, 15 cm air

gap, 18 ga. blunted needle, and 0.3 ml/h flowrate. A typical spinning run used 5 ml of solution and a round collecting mandrel (6.5 mm diameter). Scaffolds were dried under vacuum 3 hours to remove residual solvent before any further testing.

Table 1: The effect of electrospinning parameters on the size of the nanofiber. (PVA)

Effect of flow rate		Effect of distance		Effect of Volt	
Flow rate (mL h−1)	Size (nm)	Distance (cm)	Size (nm)	Voltage (kV)	Size (nm)
0.3	416±102	5	455±108	10	410±115
0.5	206±112	10	312±156	20	356±123
0.7	516±251	15	154±253	30	194±147
0.9	605±62	20	645±45	50	173±125

Table 2: The effect of electro spinning parameters on the size of the nanofiber. (PEO)

Effect of flow rate		Effect of distance		Effect of Volt	
Flow rate (mL h−1)	Size (nm)	Distance (cm)	Size (nm)	Voltage (kV)	Size (nm)
0.3	212±	5	124±108	10	545±115
0.5	172±	10	655±156	20	327±123
0.7	450±	15	219±253	30	453±147
0.9	371±	20	197±45	50	255±125

OPTIMIZATION:[15]

Generally, the design and optimization of the formulations is the crucial step after QbD. In this study, the nanosponge formulations were designed using 3^2,factorial design with the added center and axial points in the Response Surface Methodology (RSM) by Design Expert-7. Various concentrations of PVA (A) and PEO (B) were employed as control variables (process parameters).Drug Entrapment efficiency (EE %) (Y1) and Swelling index (SI) (Y2) were considered dependent variables. All the possible combinations of formulations were prepared by considering levels-1 and+1 for both controlled variables.

Table 3: Formulation table of nanofiber (Optimized)

Formulation Batches	PVA(mg/ml)	PEO(mg/ml)
BDRNF1	6.00	14.00
BDRNF2	10.00	6.00
BDRNF3	14.00	6.00
BDRNF4	14.00	10.00
BDRNF5	6.00	10.00
BDRNF6	14.00	14.00
BDRNF7	10.00	10.00
BDRNF8	6.00	6.00
BDRNF9	10.00	14.00

Table 4: Levels of independent variables with their transformed values in the preparation of nanofiber.

Independent Variables	Unit	Low Actual	High Actual	Low Coded	High Coded
PVA of (A)	mg/ml	6	14	-1.000	1.000
PEO (B)	mg/ml	6	14	-1.000	1.000

Table 5: Model fitting with DEE and SI for nanofiber.

Response	Name	Units	Analysis	Minimum	Maximum	Mean	Std. Dev.	C.V%	Model
Y1	DEE	%	Polynomial	73.19	85.12	80.12	1.23	1.54	Quadratic
Y2	Swelling index(SI)		Polynomial	65.14	86.6	77.20	2.61	3.38	Quadratic

A. Evaluation of Nanofiber

a) Drug entrapment efficiency and Drug loading (%)[16]

The ultra-centrifugation technique was used to assess the drug entrapment effectiveness of silver Nanofiber formulations. Using ultracentrifugation at 10,000 rpm for 30 minutes, AgNO3 containing the silver Nanofiber was separated from the silver Nanofiber. The pellets were re-dissolved in distilled water, and the supernatant was scanned with a UV-visible spectrophotometer in this parameter.

The drug encapsulation efficiency was determined by using the relation in this equation.

% Drug entrapment efficiency= experimental drug contentx100/Theoretical drug content

% Drug Loading = (Total drug - Free drug/ Nanosponge weight) X 100

b) **Swelling index [17]**

Swelling capacity of the nanofiber samples was investigated by direct immersion of formulations in PBS (pH 7.4) to simulate medium conditions [14]. The swelling degree (S) was calculated according to

Eq 1 [15]. $S (\%) = \{(wt - wd)/wd\}\ 100$ ………………. (1)

Where Wt is the weight of the swollen sample at time t and Wd is the initial weight of the dry sample.

c) **Scanning electron microscope (SEM) [18]**

The Scanning electron microscope (SEM, Zeiss, Japan) was used to observe the morphology and diameter of the PVA, PVA/SS, PVA/C/SS, PVA/SF and PVA/C/SF electrospun nanofiber. In this study the samples image were captured at the accelerating voltage of 5 kV under the magnification of 17.42 X. The synthesized nanofiber were cut into small pieces and coated on a gold sputter (sputter coater: Emitech SC7620) in order to prevent charging and improve the resolution of the image. The average fiber diameter was measured with the SEM images.

CHARACTERIZATION OF OPTIMIZED BATCH

1. **FTIR [19]**

FTIR spectroscopy was used in the range 400-4000 cm-1 to determine the type of functional groups on the prepared nanofiber. Dried nanofiber were mixed with KBr powder and pelletized. The IR characterizations were performed using a Perkin-Elmer Spectrum GX FTIR spectrometer.

2. **DSC [20]**

DSC has been anticipated to be a speedy and reliable technique for appraising Physico-chemical interactions between components of the formulation through the appearance, shift, or disappearance of endo- or exothermal effects and/or variations in the relevant enthalpy values. The solid-state properties of the fabricated nanofiber samples were studied using differential scanning Calorimetry (DSC 822, Mettler Toledo). Each powdered sample (5 mg) was placed in an aluminum pan, sealed, and heated to 200 ° C at a heating ramp rate of 10 ° C / min under nitrogen gas (50 L/min). Before each measurement, the sample was allowed to equilibrate for 5 min at 30 ° C. Transition temperatures and enthalpy readings were automatically calculated using Mettler Toledo software for each peak.

3. **XRD[21]**

X-Ray diffraction is a useful tool to get the structural information of crystalline compounds. Each signal in XRD represents the plane of a crystal. The structural composition can be studied using X-ray diffraction method.The samples of nanofibers were assessed for crystallinity using an X-ray diffractometer (Model: SEIFERT, C-3000, Germany) using Nickel-filtered CuKa radiation (k = 1.54 A°). The voltage and current were 35 kV and 30 mA, respectively, and smoothed 95. Measurements were carried out in the angular range from 5° to 40° (2θ) using step sizes 0.05 and 0.25 s per step.

4. TGA [22]

The thermal stability and the fraction of the volatile components of the synthesized nanofibers (PVA, PVA/SS, PVA/C/SS, PVA/SF and PVA/C/SF) were analyzed with the help of Thermo Gravimetric Analyzer (TGA) (PERKIN – ELMER TG – DTA). The samples were heated at constant heating rate at 10°C / min from room temperature to 800°C under nitrogen (N_2) atmosphere at a purging rate of 100 ml / min. During the process the weight of the samples were measured, it was not degraded, no change in weight during the desired temperature of the polymer and also no slope was observed in the TGA graph with negligible changes of the samples. If the samples were degraded the weight will decrease and if the weight will increase because the samples were reacted with oxygen.

Formulation of Wound Dressing

PREPARATION AND CHARACTERIZATION OF WOUND DRESSINGS

1. Preliminary formulation development[23]

Production of the Chitosan/alginate membrane dressings

Chitosan polyelectrolyte membranes were synthesized using physical blending and covalent crosslinking via solution casting-solvent evaporation technique.

Procedure-

1. A solution of chitosan 3 wt. % was prepared by dispersing 3 g of chitosan in 200 ml of 2% glacial acetic acid solution.

2. Then, the solution was mixed with alginate or activated alginate solution in the molar ratio of 4:1, 3:1, 2:1, and 1:1. Next, pH of the mixture was adjusted to 5.5 by adding a drop of HCl (0.05 mL) with stirring for 30 min at room temperature.

3. To this solution added 0.2 ml of formulated Optimised formulation (BRNF7).

4. A solution was slowly cast onto a clean glass plate with bubble-free and allowed to dry in the atmosphere at room temperature.

5. Both physically and covalently crosslinked CS/Alg membranes were split off from the petri dish and washed with methanol for 4–5 times, followed by vacuum drying for 5 h at 40 °C in a closed oven.

6. Membranes so formed were dense, and their thicknesses were estimated with a micrometer. Schematic diagram describes the mechanism of synthesis both covalent and ionic cross-linked CS/Alg membranes.

Table 6: Formulae for wound dressing preparation of Optimized formulation (BRNF7)

Sr. no.	Ingredients	Formulation code			
		F1	**F2**	**F3**	**F4**
1.	Chitosan: Sod. alginate	4:1	3:1	2:1	1:1
2.	Optimised formulation (BRNF7) (ml)	0.2	0.2	0.2	0.2

Characterization of wound dressings
Film Thickness *[24]*

The thickness was assessed using a thickness gauge. The sample was laid on a solid base and fitted with the probe of the thickness gauge. The thickness was measured both in dry and wet conditions (intervals of 15 min, 1 h, 3 h, 8 h, and 24 h). The measurements were made at 30 locations over the area of the sample.

Film weight and uniformity of mass [25]

The uniformity of mass evaluation for film wound dressings is not defined in *European Pharmacopoeia*. For this reason, the evaluation of the films was done according to the adapted test (2.9.5. Uniformity of mass of single-dose preparations) described in *European Pharmacopoeia*. Twenty pieces, each 2.5 × 2.5 cm in size, were rigorously cut from random locations on the prepared films. Each sample was weighed on an analytical scale (KERN 870–13, Gottl. KERN &Sohn GmbH, Germany) with an accuracy of 4 decimal places, and the average mass ± SD was assessed. The percentage of deviation from the average mass was calculated. Limits for film-coated and uncoated tablets with an average mass between 80 and 250 mg were applied (even for samples with a weight under 80 mg). According to *European Pharmacopoeia*, no more than 2 of the individual masses could deviate from the mean by more than 7.5%, and none by more than twice that percentage. Results are presented as mean values, with the minimum and maximum values expressed in mg and % of film weight.

Surface pH [26]

The surface pH of the prepared films was measured using a contact pH meter (Flatrode, Hamilton, CH) after wetting with a drop of purified water. This measurement was conducted three times for each sample, and the results are presented as average values and SDs

Drug Content uniformity [27]

Drug content uniformity was determined by dissolving the film (10 mm in diameter) from each batch by homogenization in 100 ml of an isotonic phosphate buffer (pH 6.8) for 6 h under occasional shaking. The 5ml solution was taken and diluted with isotonic phosphate buffer pH 6.8 up to 20 ml, and the resulting solution was filtered through a 0.45 mm Whatman filter paper. The drug content was then determined after proper dilution at 340nm using an UV-visible spectrophotometer.

% Drug Content= Experimental drug content/Theoretical drug content*100

In Vitro Drug Release [28]

In vitro drug release studies were performed using an Automated Transdermal Diffusion Cells Sampling System (DBK Instruments). The drug loaded samples were cut into 1 × 1 cm squares and placed on the top of a cellulose acetate membrane. The receptor compartment was filled with ultra-pure water and its temperature was maintained at 37 °C. During the dissolution testing the medium was stirred continuously with a magnetic bar. Samples were collected over a period of 24 h at different time intervals, while the released/dissolved DCF concentration in the receptor medium was determined by UV-Vis spectrophotometer (Jasco Spectrophotometer,) by quantification of the absorption band at 340 nm.

Antibacterial Activity Analysis[29]
Name of test:
Antimicrobial activity of test material by Agar Well Diffusion
Materials and methods:
Test Samples: Dressing Films
Media:
Nutrient Agar for Bacterial cultures and Chloramphenicol Yeast Glucose Agar forfungal cultures
Cultures against which activity was tested (Cultures used):
Bacterial cultures: B. subtilis NCIM 2063,
S. aureus NCIM 2079,
E. coli NCIM 2065,
P. vulgaris NCIM 2813
Fungal Culture: A. niger NCIM 501,
C. albicans NCIM 3471
Incubation temperature: 37°C
Incubation time: 24 Hrs.
The Agar Well Diffusion Method carried out the antibacterial operation of the dressing films.

1. A 24-hour culture has been separately prepared for B. subtilis NCIM 2063, S. aureus NCIM 2079, E. coli NCIM 2065, P. vulgaris NCIM 2813, A. niger NCIM 501 and C. albicans NCIM 3471.
2. Sterile Nutrient Agar Plates were prepared for bacterial cultures and sterile Chloramphenicol Yeast Glucose Agar was prepared for fungal cultures.
3. With sterile swabson distinct plates, a 0.2 ml culture of each type of micro-organism was distributed.
4. Four or five wells were prepared with one plate of 8.0 mm cork borer in the agar.
5. Dimethyl sulfoxide (DMSO) was prepared as a stock solution for a 10 mg/ml suspension of the test material.
6. In each well, 50 µl of the stock solution was injected. As normal, cisplatin was used at 0.5 mg/ml (Std).
7. The plates were incubated for 24 hours at 37°C. The region of inhibition was assessed in millimetres after incubation (mm).

Wound healing activity[30-31]
Species and Strain: Albino Rabbit
Age and Weight: Weight range: 200-240 g.(12-16 weeks)
Gender: Either sex

Table 7: Dose & No. of animals used

Sr No	Name of group	Treatment	No. of animals
1	Normal group	Tween 80	6
2	Standard	Drug	6
3	Dressing formulations (4)	Dressings	24

Procedure:

1. Swiss–albino Rats weighing between 25 to 30 g will be used in this study.
2. Animals will be kept in a separate animal room, in a 12 h light/dark cycle (with lights on at 6:00 a.m.), at a room temperature of 22 ± 2 °C, with free access to water and standard diet ad libitum.
3. Rats will be anesthetized by subcutaneous injection of chloral hydrate (1 mL/kg) and 1% atropine. The back of the Rats will be further shaved.
4. A 215 mm2 (representing 3.2% of the weight of Rats) circular area will be marked and the surface of the marked area will be carefully excised by using sharp sterilized scissors.
5. After 24 h of wound creation, the wound dressings will be gently applied to cover the wounded area once per day until reaching complete healing.
6. Wound area, wound contraction, epithelialization period, and hydroxyproline content were monitored during the whole healing process.

RESULT AND DISCUSSION:

Characterization of nanofiber

a) Drug entrapment efficiency

Table 8: Determination of Entrapment efficiency (%) of nanofiber BDRNF1-BDRNF9

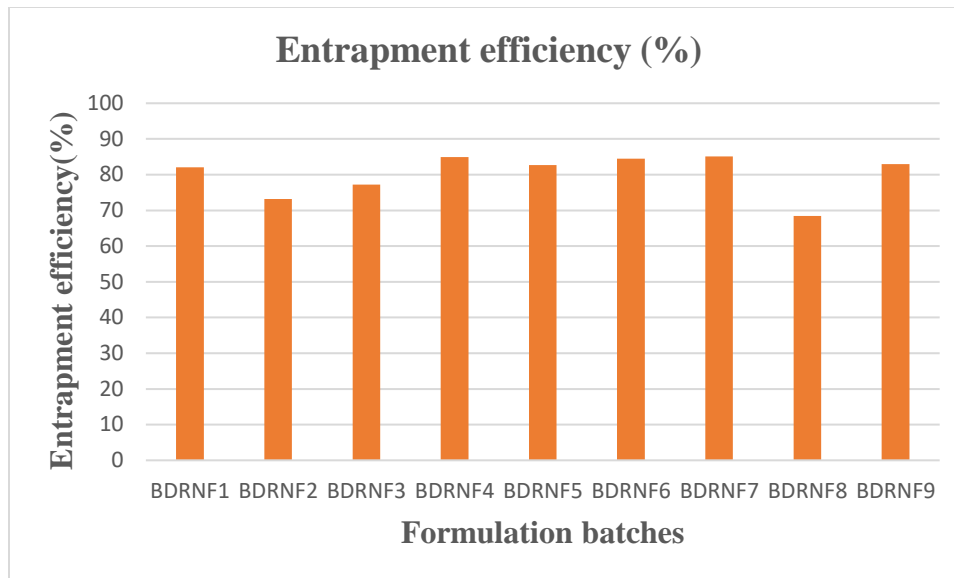| Sr. no	Formulation	Entrapment efficiency (%)
1.	**BDRNF1**	82.02
2.	**BDRNF2**	73.19
3.	**BDRNF3**	77.2
4.	**BDRNF4**	84.97
5.	**BDRNF5**	82.66
6.	**BDRNF6**	84.52
7.	**BDRNF7**	85.12
8.	**BDRNF8**	68.45
9.	**BDRNF9**	82.96

Entrapment efficiency (%)

Figure 1: Determination of Entrapment efficiency (%) of nanofiber BDRNF1-BDRNF9

Discussion: Percent entrapped drug and free drug percentage of nanofiber was determined using the UV spectrophotometric. The entrapment efficiency was found to be increased with concentration of polymer increase. Batch BDRNF4 and BDRNF57shows higher drug entrapment efficiency which provides optimum availability of drug at site without any side effects. BDRNF7 optimized batches show 85.12% entrapment efficiency as compared to other batches

ANOVA for Quadratic model

Response 1: DEE

Table 9:Response DEE

Source	Sum of Squares	df	Mean Square	F-value	p-value	
Model	274.21	5	54.84	36.24	0.0070	significant
A-PVA	30.65	1	30.65	20.25	0.0205	
B-PEO	156.67	1	156.67	103.52	0.0020	
AB	9.77	1	9.77	6.45	0.0847	
A²	0.4110	1	0.4110	0.2716	0.6383	
B²	76.71	1	76.71	50.69	0.0057	
Residual	4.54	3	1.51			
Cor Total	278.75	8				

Factor coding is **coded**.
Sum of squares is **Type III - Partial**

The **Model F-value** of 36.24 implies the model is significant. There is only a 0.70% chance that an F-value this large could occur due to noise.

P-values less than 0.0500 indicate model terms are significant. In this case A, B, B² are significant model terms. Values greater than 0.1000 indicate the model terms are not significant. If there are many insignificant model terms (not counting those required to support hierarchy), model reduction may improve your model.

Fit Statistics

Table 10:Fit Statistics

Std. Dev.	1.23	R²	0.9837
Mean	80.12	Adjusted R²	0.9566
C.V. %	1.54	Predicted R²	0.8138
		Adeq Precision	17.3085

The **Predicted R²** of 0.8138 is in reasonable agreement with the **Adjusted R²** of 0.9566; i.e. the difference is less than 0.2.

Adeq Precision measures the signal to noise ratio. A ratio greater than 4 is desirable. Your ratio of 17.309 indicates an adequate signal. This model can be used to navigate the design space.

Final Equation in Terms of Coded Factors

Table 11:Final Equation in Terms of Coded Factors

DEE	=
+84.55	
+2.26	A
+5.11	B
-1.56	AB
-0.4533	A²
-6.19	B²

The equation in terms of coded factors can be used to make predictions about the response for given levels of each factor. By default, the high levels of the factors are coded as +1 and the low levels are coded as -1. The coded equation is useful for identifying the relative impact of the factors by comparing the factor coefficients.

Final Equation in Terms of Actual Factors

Table 12:Final Equation in Terms of Actual Factors

DEE	=
+14.81993	
+2.10823	PVA

+9.99573	PEO
-0.097656	PVA * PEO
-0.028333	PVA²
-0.387083	PEO²

The equation in terms of actual factors can be used to make predictions about the response for given levels of each factor. Here, the levels should be specified in the original units for each factor. This equation should not be used to determine the relative impact of each factor because the coefficients are scaled to accommodate the units of each factor and the intercept is not at the center of the design space.
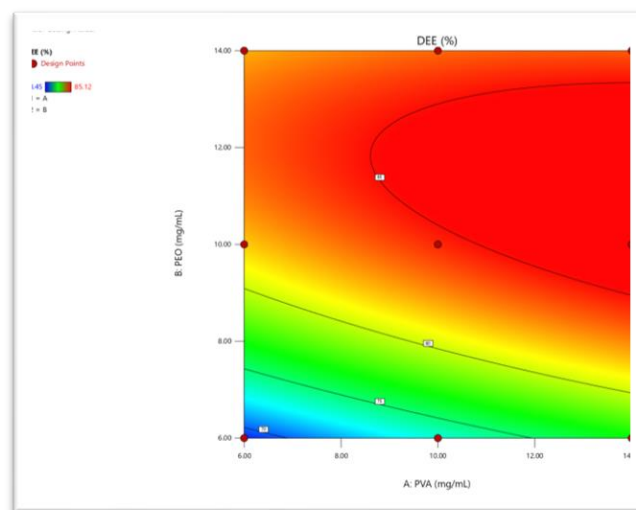
Figure 2: counter plot of drug entrapment efficiency

B) Drug Loading of nanofiber:

Table 13: Determination of Drug loading (%) of nanofiber BDRNF1-BDRNF9

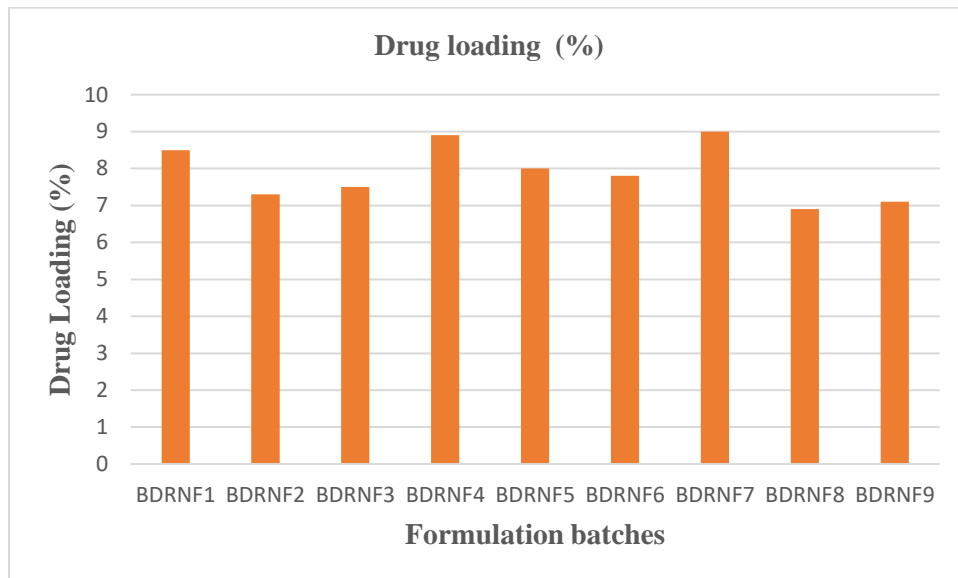| Sr. no	Formulation	Drug loading (%)
1.	BDRNF1	8.5
2.	BDRNF2	7.3
3.	BDRNF3	7.5
4.	BDRNF4	8.9
5.	BDRNF5	8.0
6.	BDRNF6	7.8
7.	BDRNF7	9
8.	BDRNF8	6.9
9.	BDRNF9	7.1

Figure 3: Determination of Drug loading (%) of nanofiber BDRNF1-BDRNF9

Discussion:

The optimized batch BDRNF7 with 9% drug loading provide valuable information for potential drug delivery application

c) Swelling index

Table 14: Swelling index

Sr. no	Formulation	Swelling (%)
1.	BDRNF1	65.14
2.	BDRNF2	72.08
3.	BDRNF3	75.55
4.	BDRNF4	85.23
5.	BDRNF5	77.91
6.	BDRNF6	83.62
7.	BDRNF7	86.6
8.	BDRNF8	69.86
9.	BDRNF9	78.82

The swelling index of the electrospun nanofiber materials was determined using a gravimetric method. The swelling index of the nanofiber plays an important role in the loading and release behavior of a drug. Above figure shows the degree of swelling of drugloaded nanofiber gel at different time intervals. The degree of swelling of Nano fibrous gel (BDRNF1-BDRNF9) in PBS pH 7.4 65.14, 72.08, 75.55, 85.23, 77.91, 83.62, 86.6, 69.86 was and 78.82 for the time intervals of 1, 2, 4, 6, 8, 10, and 12 h, respectively.

ANOVA for Quadratic model

Response 2: SI

Table 15: Response of swelling index

Source	Sum of Squares	df	Mean Square	F-value	p-value	
Model	404.99	5	81.00	11.88	0.0343	significant
A-PVA	165.27	1	165.27	24.24	0.0161	
B-PEO	16.97	1	16.97	2.49	0.2128	
AB	40.90	1	40.90	6.00	0.0917	
A²	17.39	1	17.39	2.55	0.2086	
B²	164.47	1	164.47	24.12	0.0162	
Residual	20.45	3	6.82			
Cor Total	425.44	8				

Factor coding is **coded**.
Sum of squares is **Type III - Partial**

The **Model F-value** of 11.88 implies the model is significant. There is only a 3.43% chance that an F-value this large could occur due to noise.

P-values less than 0.0500 indicate model terms are significant. In this case A, B² are significant model terms. Values greater than 0.1000 indicate the model terms are not significant. If there are many insignificant model terms (not counting those required to support hierarchy), model reduction may improve your model.

Fit Statistics

Table 16:Fit Statistics

Std. Dev.	2.61		R²	0.9519
Mean	77.20		**Adjusted R²**	0.8718
C.V. %	3.38		**Predicted R²**	0.4623
			Adeq Precision	9.8881

The **Predicted R²** of 0.4623 is not as close to the **Adjusted R²** of 0.8718 as one might normally expect; i.e. the difference is more than 0.2. This may indicate a large block effect or a possible problem with your model and/or data. Things to consider are model reduction, response transformation, outliers, etc. All empirical models should be tested by doing confirmation runs.

Adeq Precision measures the signal to noise ratio. A ratio greater than 4 is desirable. Your ratio of 9.888 indicates an adequate signal. This model can be used to navigate the design space.

Final Equation in Terms of Coded Factors

Table 17:Final Equation in Terms of Coded Factors

SI	=
+85.21	
+5.25	A
+1.68	B
+3.20	AB
-2.95	A²
-9.07	B²

The equation in terms of coded factors can be used to make predictions about the response for given levels of each factor. By default, the high levels of the factors are coded as +1 and the low levels are coded as -1. The coded equation is useful for identifying the relative impact of the factors by comparing the factor coefficients.

Final Equation in Terms of Actual Factors

Table 18:Final Equation in Terms of Actual Factors

SI	=
+12.76743	
+2.99906	PVA
+9.75740	PEO
+0.199844	PVA * PEO
-0.184271	PVA²
-0.566771	PEO²

The equation in terms of actual factors can be used to make predictions about the response for given levels of each factor. Here, the levels should be specified in the original units for each factor. This equation should not be used to determine the relative impact of each factor because the coefficients are scaled to accommodate the units of each factor and the intercept is not at the center of the design space.
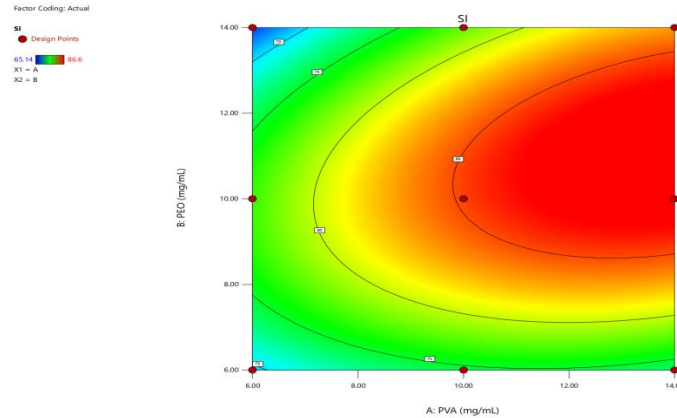
Figure 4: counter plot of drug loading

D) Scanning electron microscope (SEM)

Particle shape and its arrangement inside the formulation can be unfolded by scanning electron microscopy (SEM). Scanning electron microscopy was used to examine the surface morphology of silver nanofiber. The SEM graphs are represented below. The morphology for plain and prepared nanofiber patches was analyses by using a Hitachi S-4700 SEM (scanning electron in Hitachi Company, Japan). Before being considered, samples were placed on metal ends using double-sided adhesive tape and vacuum-coated with a gold sputter layer.
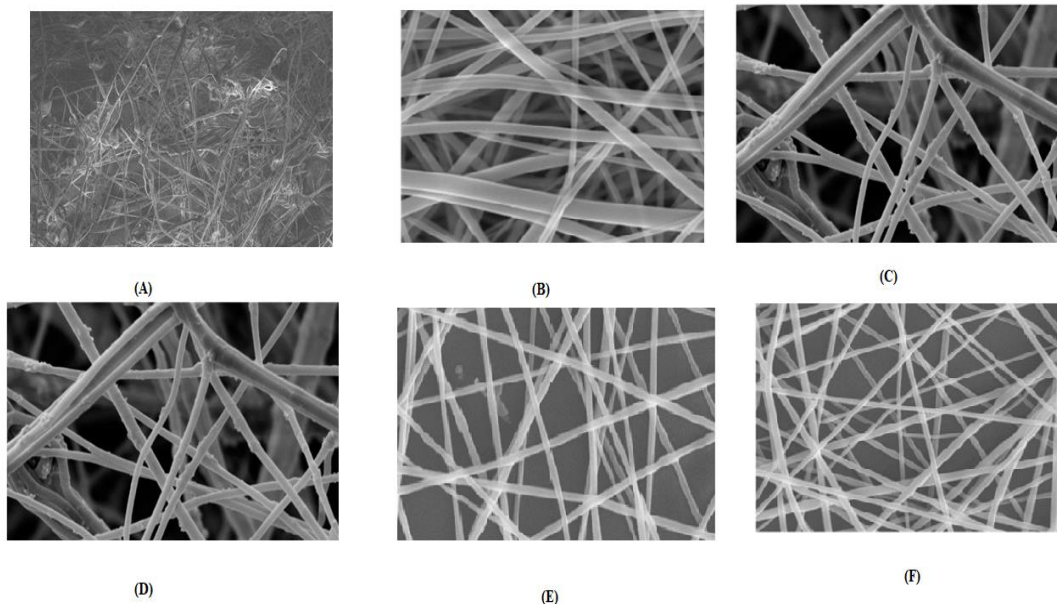

Figure 5: A- Scanning electron microscopy (BDRNF1), B- Scanning electron microscopy (BDRNF2), C- Scanning electron microcopy (BDRNF3), D- Scanning electron microscopy (BDRNF4), E- Scanning electron microscopy (BDRNF5), F-Scanning electron microscopy (BDRNF6).
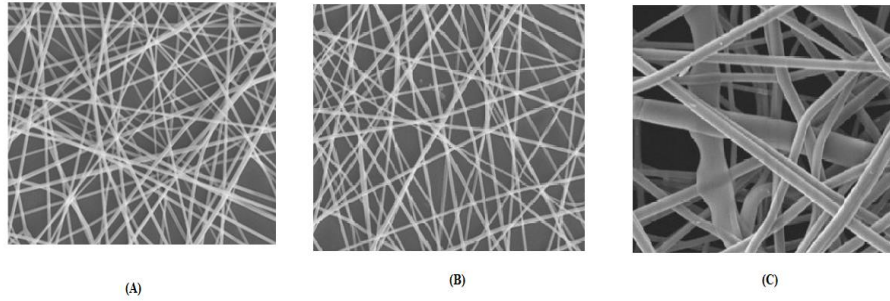
(A)   (B)   (C)

Figure 6:A- Scanning electron microscopy (BDRNF7),B- Scanning electron microscopy (BDRNF8),C- Scanning electron microscopy (BDRNF9)

Characterization of optimized batch

a) **FTIR:**

Table 19: FTIR interpretation of optimized nanofiber batch (BDRNF7)

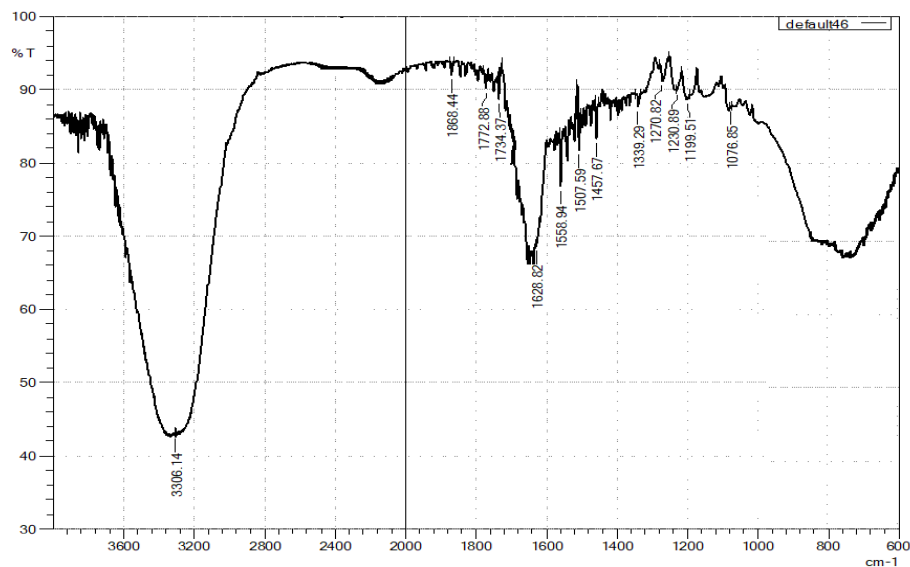| Functional Group	Vibrational Frequency (cm−1)
O-H stretch	3306.14
C=O stretch	1628.82
Alkene (C-H stretch)	1457.67
Esters (C–O stretch)	1076.85

Figure 7: IR spectrum of prepared nanofiber batch BDRNF7
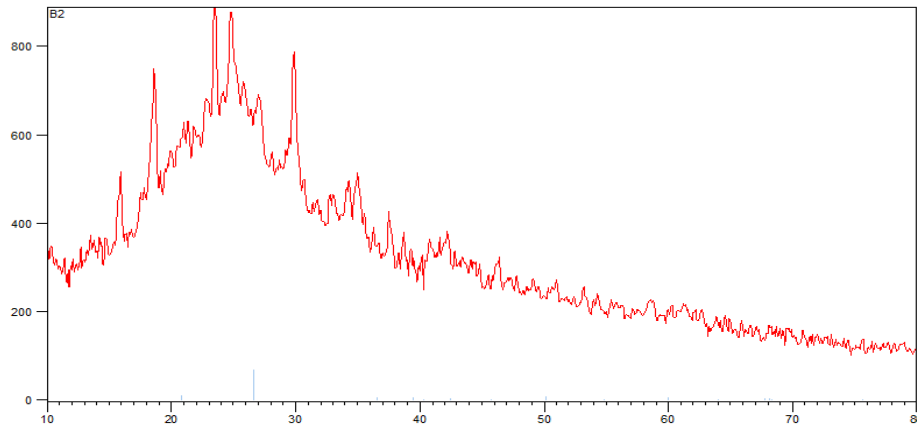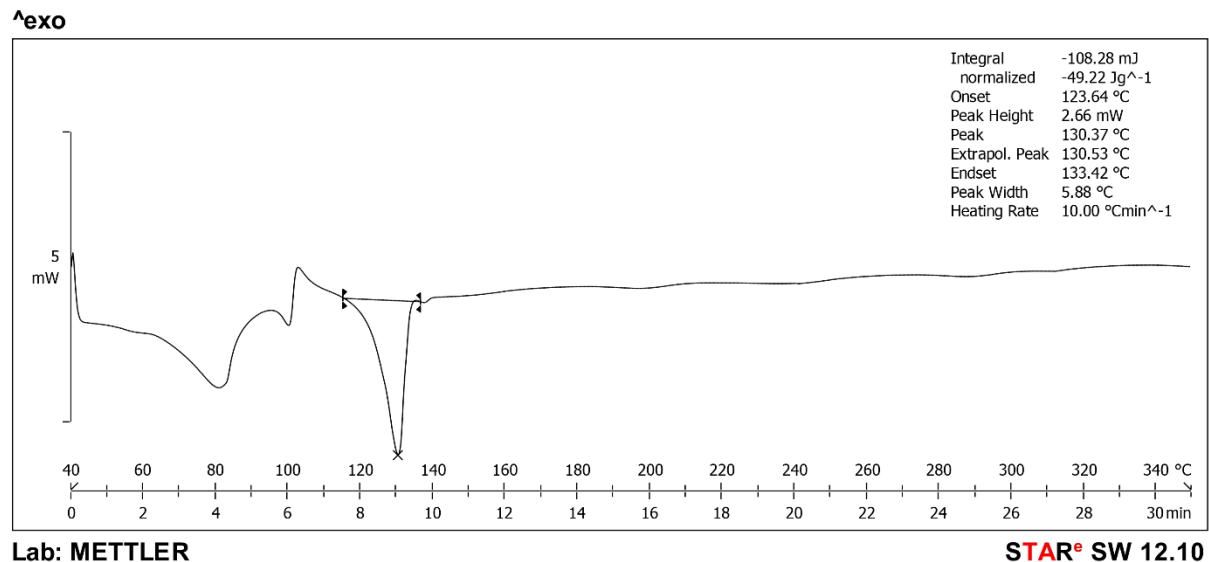
b) XRD:

Figure 8: XRD spectrum of prepared nanofiber batch BDRNF7

Discussion: X-Ray diffraction is a useful tool to get the structural information of crystalline compounds. Each signal in XRD represents the plane of a crystal. Spectra of optimized batch (BDRNF7) revealed intense peaks, which indicates crystalline structure.

c) DSC:

Figure 9: DSC spectrum of prepared nanofiber batch BDRNF7

Integral	-108.28 mJ
normalized	-49.22 Jg^-1
Onset	123.64 °C
Peak Height	2.66 mW
Peak	130.37 °C
Extrapol. Peak	130.53 °C
Endset	133.42 °C
Peak Width	5.88 °C
Heating Rate	10.00 °Cmin^-1

Lab: METTLER **STAR^e SW 12.10**

Discussion:

The DSC spectrum of prepared nanofiber batch BDRNF7 prepared nanofiber batch BDRNF7 showing end set of 133.42°C, which is quite excess when compared with the end set temperature of crude powder melting point of Boerhavia diffusa.
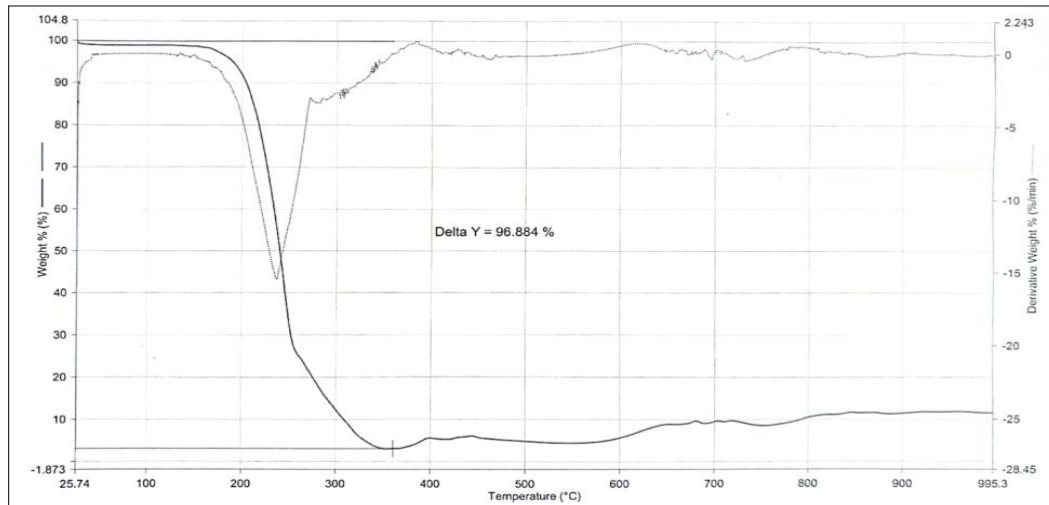
d) TGA:

Figure 10: TGA spectrum of prepared nanofiber batch BDRNF7

Discussion:

TGA thermograms of the prepared nanofiber batch BDRNF7show that the nanofiber gradually decomposed at a higher temperature range.

CHARACTERIZATION OF WOUND DRESSINGS

Film Thickness

Table 20: Thickness of Boerhavia diffusa extract loaded Nanofibrous dressing

Formulation	Thickness
B1	0.069±1.20
B2	0.072±1.45
B3	0.073±1.30
B4	0.074±1.80

The thickness of the film B1 and B4 was found to be in range of 0.069 to 0.074. In all cases, calculated standard deviation values are low which indicates that proposed films were uniform in thickness.

Folding endurance

Table 21: Folding endurance of Boerhavia diffusa extract loaded Nanofibrous dressing

Formulation	Folding endurance
B1	302
B2	304
B3	310
B4	308

The folding endurance of all the films was given above table. All the films, irrespective of polymers used, showed good folding endurance, thereby ensuring good flexibility.

Percent moisture absorption

Table 22: Results of Percent moisture absorption

Formulation	Percent moisture absorption
B1	3.9
B2	4.1
B3	3.8
B4	4.6

Moisture interaction studies are necessary to find out the physical stability of the film at high humid conditions and integrity of the film at dry conditions. The percent moisture absorption study was done over a period of 3 days and the results were found to be varied between 3.8% to 4.6%.

Percent moisture loss

Table 23:Percent moisture loss

Formulation	Percent moisture loss
B1	3.2
B2	3.9
B3	2.7
B4	4.7

The results of percent moisture loss varied between 3.2% to 4.7% as shown in Table.

Film weight and uniformity of mass

Table 24: Weight variation of wound dressings

Formulation	Weight (mg)
B1	23.45±0.14
B2	25.14±1.04
B3	27.48±1.23
B4	28.04±1.47

No significant variation in the average weight was observed for the developed films.

Tensile Strength

Table 25: Tensile strength of Boerhavia diffusa extract loaded Nanofibrous dressing

Formulation	Tensile strength (Kg/cm^2)
B1	2.15
B2	2.56
B3	2.14
B4	2.85

Tensile strength value of developed formulations was in between 2.14-2.85kg/cm2.

Drug Content uniformity

Table 26: Drug content estimation of Boerhavia diffusa extract loaded Nanofibrous dressing

Formulation	Drug content (%)
B1	90.15±1.56
B2	91.78±1.47
B3	92.11±1.56
B4	91.98±1.78

Percentage drug content for all the patches was in between 90.15-92.11%. It was observed from the drug content data that there was no significance difference in uniformity of the drug content.

***W*ater vapor permeability**

In Vitro Drug Release

Table 27: In-vitro diffusion data

Time in hr	% cumulative drug release			
	B1	**B2**	**B3**	**B4**
0	0	0	0	0
1	11.45	12.45	17.45	16.23
2	26.89	31.26	30.14	29.87
3	47.48	50.12	47.89	49.55
4	67.59	62.45	69.56	67.44
5	72.65	74.59	74.22	75.45
6	80.45	81.15	82.12	82.97
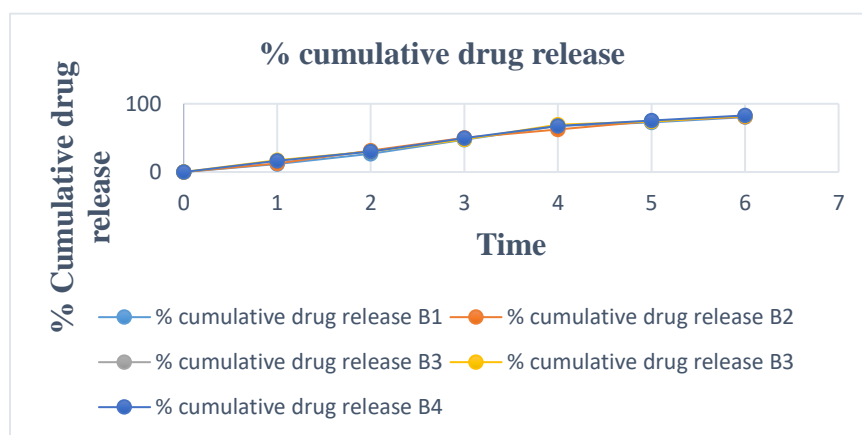
Figure 11:% cumulative drug release

Antibacterial Activity Analysis

Antibacterial activity against Bacillus subtilis NCIM 2063, Staphylococcus aureus NCIM 2079, Escherichia coli NCIM 2065, Proteus vulgaris NCIM 2813, Aspergillus niger NCIM 501 and Candida albicans NCIM 3471 in terms of Zone of inhibition in mm is presented below.
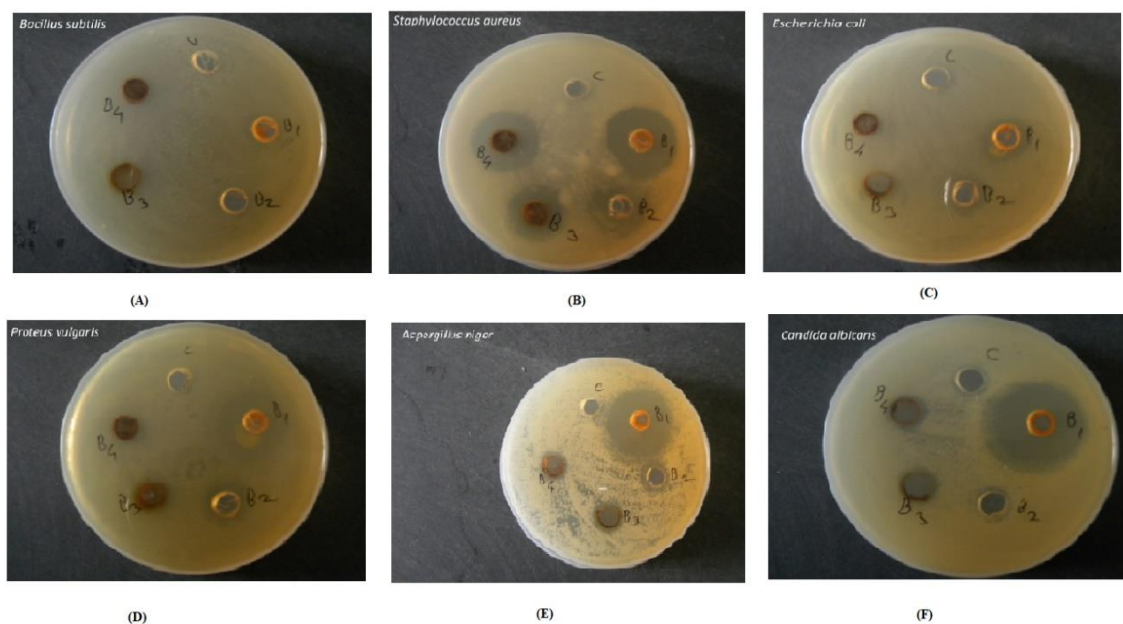

Figure 12: A- Microbial activities against *Bacillus subtilis* (B1 to B4), B- Microbial activities against *Staphylococcus aureus* (B1 to B4), C- Microbial activities against *Escherichia Coli* (B1 to B4), D- Microbial activities against *Proteus valgaris* (B1 to B4), E- Microbial activities against *Aspergillus Niger* (B1 to B4), F- Microbial activities against *Candida albicans* (B1 to B4)

Table. Antimicrobial Activity wound dressings

Sample ID	Conc. of Stocksolution	Zone of inhibition in mm					
		Bacillus subtilis NCIM 2063	*Staphylococcus aureus* NCIM 2079	*Escherichia coli* NCIM 2065	*Proteus vulgaris* NCIM 2813	*Aspergillus niger* NCIM 501	*Candida albicans* NCIM 3471
B1	**10mg/ml**	9	15	12	10	23	30
B2		4	19	12	9	24	30
B3		9	12	12	11	20	28
B4		8	11	10	13	18	29
Std.	**0.5mg/ml**	18	23	17	18	28	33

Percent wound contraction area on different days for control and Wound Dressing
Wound healing activity

Table 28: Wound-healing effect of Boerhavia diffusa extract loaded Nanofibrous dressing

Parameter	Wound area (mm2) and percentage of wound contraction				
Post-wounding Days	Control	B1	B2	B3	B4
Day 0	440.66 ± 2.6757	440 ± 2.1581	440.66 ± 2.1689	503 ± 3.2151	505.66 ± 2.1554
Day 2	428.26 ± 3.1528 (4.24%)	432.66 ± 1.202 (5.47%)	435.33 ± 1.3855* (7.35%)	469.66 ± 1.202 (6.62%)	465.33 ± 1.3335* (7.97%)
Day 4	468.33 ± 1.3336 (15.55%)	324.33 ± 0.589** (21.80%)	384.1 ± 2.714** (27.61%)	393.33 ± 0.989** (21.80%)	366 ± 2.7814** (27.61%)
Day 8	324 ± 1.1549 (32.89%)	285.66 ± 1.545** (40.81%)	289.66 ± 1.641** (42.86%)	292.66 ± 1.3335** (41.81%)	268.66 ± 1.7641** (46.86%)
Day 12	204.66 ± 1.162 (52.47%)	156 ± 1.478** (62.19%)	125 ± 1.218** (71.27%)	165 ± 1.5278** (67.19%)	125 ± 1.3418** (75.27%)
Day 16	77.33 ± 1.4691 (84.64%)	38 ± 1.1549** (95.62%)	17.38 ± 1.202** (97.29)	22 ± 1.1549** (95.62%)	13.66 ± 1.202** (97.29)
Day 18	24.33 ± 1.202 (95.16%)	5.28 ± 0.9546** (98.87%)	00 ± 00** (100%)	5.66 ± 0.9546** (98.87%)	00 ± 00** (100%)
Day 20	9 ± 0.5465 (93.21%)	00 ± 00** (100%)	00 ± 00** (100%)	00 ± 00** (100%)	00 ± 00** (100%)
Period of epithelialization (day)	25.5 ± 0.7416	18.33 ± 0.3058**	17.16 ± 0.7846**	18.33 ± 0.2108**	17.16 ± 0.1666**

$n = 6$, values are expressed as mean ± SEM; *$P < 0.01$; **$P < 0.001$ significant
as compared with control;

Table 29: Wound-healing effect of Boerhavia diffusa extract loaded Nanofibrous dressing

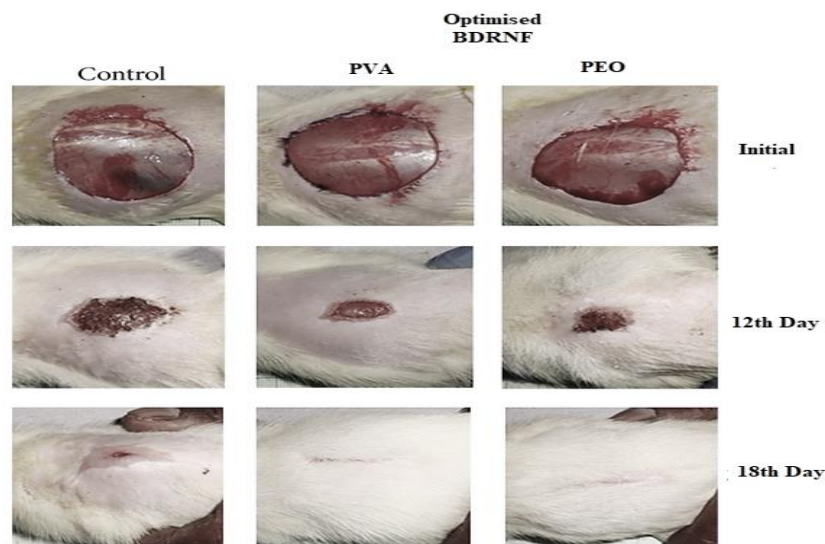| Parameter	Control	B1	B2	B3	B4
Skin breaking strength	275.5 ± 2.2274	266.66 ± 2.5344*	296.66 ± 2.459*	447.66 ± 2.7044*	466.66 ± 2.459*

Figure 13: Wound-healing effect of Boerhavia diffusa extract loaded Nanofibrous dressing

Reference:

1. Malabadi RB, Kolkar KP, Acharya M, Nityasree BR, Chalannavar RK. Wound Healing: Role of Traditional Herbal Medicine Treatment. International Journal of Innovation Scientific Research and Review. 2022; 4(6):2856-74.

2. Agarwal S, Wendorff JH, Greiner A. Use of electrospinning technique for biomedical applications. Polymer. 2008 Dec 8; 49(26):5603-21.

3. Sen CK. Human wounds and its burden: an updated compendium of estimates. Advances in wound care. 2019 Feb 1; 8(2):39-48.

4. Monika P, Waiker PV, Chandraprabha MN, Rangarajan A, Murthy KN. Myofibroblast progeny in wound biology and wound healing studies. Wound Repair and Regeneration. 2021 Jul; 29(4):531-47.

5. Gonzalez AC, Costa TF, Andrade ZD, Medrado AR. Wound healing-A literature review. Anais brasileiros de dermatologia. 2016 Sep;91:614-20.

6. Ghodela NK, Dudhamal T. Wound healing potential of Ayurved herbal and herbo-mineral formulations: A brief review. International Journal of Herbal Medicine. 2017;5(1):39-45.

7. Han G, Ceilley R. Chronic wound healing: a review of current management and treatments. Advances in therapy. 2017 Mar;34:599-610.

8. Khanam S. A systematic review on wound healing and its promising medicinal plants. IP Int J ComprAdvPharmacol. 2021 Jan 15;5:170-6.

9. Cide, Felip, José Urebe, and Andrés Revera."Exploring Monopulse Feed Antennas for Low Earth Orbit Satellite Communication: Design, Advantages, and Applications." *National Journal of Antennas and Propagation* 4.2 (2022): 20-27.

10. Gour R. BoerhaaviaDiffusa Linn Plant: A Review–One Plant with Many Therapeutic Uses. vol. 2021;6:25-41.

11. Murti K, Panchal MA, Lambole V. Pharmacological properties of Boerhaaviadiffusa-a review. Int J Pharm Sci Rev Res. 2010;5(2):107-10.

12. Bhardwaj N, Kundu SC. Electrospinning: A fascinating fiber fabrication technique. Biotechnology advances. 2010 May 1;28(3):325-47.

13. Thakkar S, Misra M. Electrospun polymeric nanofibers: New horizons in drug delivery. European Journal of Pharmaceutical Sciences. 2017 Sep 30;107:148-67.

14. Anjum S, Gupta A, Sharma D, Gautam D, Bhan S, Sharma A, Kapil A, Gupta B. Development of novel wound care systems based on nanosilvernanohydrogels of polymethacrylic acid with Aloe vera and curcumin. Materials Science and Engineering: C. 2016 Jul 1;64:157-66.

15. Eatemadi A, Daraee H, Zarghami N, MelatYar H, Akbarzadeh A. Nanofiber: Synthesis and biomedical applications. Artificial cells, nanomedicine, and biotechnology. 2016 Jan 2;44(1):111-21.

16. Park, Sehie. "All metric fixed point theorems hold for quasi-metric spaces." *Results in Nonlinear Analysis* 6.4 (2023): 116-127.

17. NOOTHI S, MALOTHU N, DESU PK, KUMAR S. IMPLICATION OF CENTRAL COMPOSITE DESIGN IN THE DEVELOPMENT OF SIMVASTATIN-LOADED NANOSPONGES. Int J App Pharm. 2023;15(5):227-36.

18. Arthanari S, Mani G, Jang JH, Choi JO, Cho YH, Lee JH, Cha SE, Oh HS, Kwon DH, Jang HT. Preparation and characterization of gatifloxacin-loaded alginate/poly (vinyl alcohol) electrospun nanofibers. Artificial cells, nanomedicine, and biotechnology. 2016 Apr 2;44(3):847-52.

19. Ye P, Wei S, Luo C, Wang Q, Li A, Wei F. Long-term effect against methicillin-resistant staphylococcus aureus of emodin released from coaxial electrospinning nanofiber membranes with a biphasic profile. Biomolecules. 2020 Feb 27;10(3):362.

20. VG R, Tambe AB, Deshmukh VK. Topical anti-inflammatory gels of naproxen entrapped in eudragit based microsponge delivery system. Journal of Advanced Chemical Engineering. 2015;5(2).

21. Pawar S, Shende P, Trotta F. Diversity of β-cyclodextrin-based nanosponges for transformation of actives. International Journal of Pharmaceutics. 2019 Jun 30;565:333-50.

22. G. Sasikala, & G. Satya Krishna. (2023). Low Power Embedded SoC Design. *Journal of VLSI Circuits and Systems*, *6*(1), 25–29. https://doi.org/10.31838/jvcs/06.01.04

23. Gangadharappa HV, Prasad SM, Singh RP. Formulation, in vitro and in vivo evaluation of celecoxib nanosponge hydrogels for topical application. Journal of Drug Delivery Science and Technology. 2017 Oct 1; 41:488-501.

24. Moin A, Roohi NF, Rizvi SM, Ashraf SA, Siddiqui AJ, Patel M, Ahmed SM, Gowda DV, Adnan M. Design and formulation of polymeric nanosponge tablets with enhanced solubility for combination therapy. RSC advances. 2020;10(57):34869-84.

25. Yang W, He X, Luzi F, Dong W, Zheng T, Kenny JM, Puglia D, Ma P. Thermomechanical, antioxidant and moisture behaviour of PVA films in presence of citric acid esterified cellulose nanocrystals. International Journal of Biological Macromolecules. 2020 Oct 15;161:617-26.

26. do AmaralSobral PJ, Gebremariam G, Drudi F, De AguiarSaldanhaPinheiro AC, Romani S, Rocculi P, Dalla Rosa M. Rheological and viscoelastic properties of chitosan solutions prepared with different chitosan or acetic acid concentrations. Foods. 2022 Sep 3;11(17):2692.

27. JONNERBY, JAKOB, A. BREZGER, and H. WANG. "Machine learning based novel architecture implementation for image processing mechanism." *International Journal of communication and computer Technologies* 11.1 (2023): 1-9.

28. Niyaz US, Elango K. Oral fast dissolving films: An innovative drug delivery system. World Journal of Pharmacy and Pharmaceutical Sciences. 2018;7(11):881-907.

29. Elsayed I, El-Dahmy RM, Elshafeey AH, Abd El Gawad NA, El Gazayerly ON. Tripling the bioavailability of rosuvastatin calcium through development and optimization of an in-situ forming nanovesicular system. Pharmaceutics. 2019 Jun 11;11(6):275.

30. Vinklárková L, Masteiková R, Vetchý D, Doležel P, Bernatonienė J. Formulation of novel layered sodium carboxymethylcellulose film wound dressings with ibuprofen for alleviating wound pain. BioMed research international. 2015 May 18;2015.

31. Omara AE, Elsakhawy T, Alshaal T, El-Ramady H, Kovács Z, Fári M. Nanoparticles: a novel approach for sustainable agro-productivity. Environment, Biodiversity and Soil Security. 2019 Feb 1;3(2019):29-62.

32. He S, Jacobsen J, Nielsen CU, Genina N, Østergaard J, Mu H. Exploration of in vitro drug release testing methods for saquinavirmicroenvironmental pH modifying buccal films. European Journal of Pharmaceutical Sciences. 2021 Aug 1;163:105867.

33. Balouiri M, Sadiki M, Ibnsouda SK. Methods for in vitro evaluating antimicrobial activity: A review. Journal of pharmaceutical analysis. 2016 Apr 1;6(2):71-9.

34. Kumar VI, Khan AA, Nagarajan K. Animal models for the evaluation of wound healing activity. Int Bull Drug Res. 2013;3(5):93-107.

35. Nasir MA, Mahammed NL, Roshan S, Ahmed MW. Wound healing activity of poly herbal formulation in albino rats using excision wound model, incision wound model, dead space wound model and burn wound model. Int. J. Res. Dev. Pharm. L. Sci. 2016;5(2):2080-7.